INTERIM REPORT

Underwater EMI Sensor Platform for Metallic Item Detection

Classification Performance of Full-Scale EMI Array

ESTCP Project MR-201610

JANUARY 2020

Daniel Steinhurst
Glenn Harbaugh
Nova Research

Grace Massey
VIMS

Thomas Bell
Leidos Corporation

ESTCP

REPORT DOCUMENTATION PAGE

Form Approved
OMB No. 0704-0188

PLEASE DO NOT RETURN YOUR FORM TO THE ABOVE ORGANIZATION.

1. REPORT DATE *(DD-MM-YYYY)*	2. REPORT TYPE	3. DATES COVERED *(From - To)*
31-Jan-2020	ESTCP Interim Report	04/01/2017 - 12/31/2019

4. TITLE AND SUBTITLE

Underwater EMI Sensor Platform for Metallic Item Detection: Classification Performance of Full-Scale EMI Array

5a. CONTRACT NUMBER

5b. GRANT NUMBER

5c. PROGRAM ELEMENT NUMBER

6. AUTHOR(S)

Daniel Steinhurst and Glenn Harbaugh, Nova Research

Grace Massey, VIMS

Thomas Bell, Leidos Corporation

5d. PROJECT NUMBER

MR-201610

5e. TASK NUMBER

5f. WORK UNIT NUMBER

7. PERFORMING ORGANIZATION NAME(S) AND ADDRESS(ES)

Nova Research, Inc.
1900 Elkin St., Ste 230
Alexandria, VA 22308;

8. PERFORMING ORGANIZATION REPORT NUMBER

MR-201610

9. SPONSORING/MONITORING AGENCY NAME(S) AND ADDRESS(ES)

Environmental Security Technology Certification Program
4800 Mark Center Drive, Suite 16F16
Alexandria, VA 22350-3605

10. SPONSOR/MONITOR'S ACRONYM(S)

ESTCP

11. SPONSOR/MONITOR'S REPORT NUMBER(S)

MR-201610

12. DISTRIBUTION/AVAILABILITY STATEMENT

DISTRIBUTION STATEMENT A. Approved for public release: distribution unlimited.

13. SUPPLEMENTARY NOTES

14. ABSTRACT

The Marine Towed Array (MTA) is an underwater dual-mode sensor array that was designed and developed over multiple years with funding under SERDP project MR-1322 and ESTCP project MR-200324. The MTA's magnetometer array has been successfully used for target detection and location at a number of underwater munitions sites. Its electromagnetic induction (EMI) array failed due to a flooded interface module in the early stages of testing and its performance was never fully evaluated. The objective of this project is to replace the existing EMI array with one based on advanced electronics and sensor designs and evaluate its classification performance. This report documents the results of our testing and analysis of the effects of array configuration on classification performance.

15. SUBJECT TERMS

Underwater EMI Sensor Platform, Metallic Item Detection, Classification Performance, Full-Scale EMI Array

16. SECURITY CLASSIFICATION OF:			17. LIMITATION OF ABSTRACT	18. NUMBER OF PAGES	19a. NAME OF RESPONSIBLE PERSON
a. REPORT	b. ABSTRACT	c. THIS PAGE			Dan Steinhurst
Unclassified	Unclassified	Unclassified	Unlimited	26	19b. TELEPHONE NUMBER *(Include area code)* 202-767-3556

Abstract

The Marine Towed Array (MTA) is an underwater dual-mode sensor array that was designed and developed over multiple years with funding under SERDP project MR-1322 and ESTCP project MR-200324. The MTA's magnetometer array has been successfully used for target detection and location at a number of underwater munitions sites. Its electromagnetic induction (EMI) array failed due to a flooded interface module in the early stages of testing and its performance was never fully evaluated. The objective of this project is to replace the existing EMI array with one based on advanced electronics and sensor designs and evaluate its classification performance. This report documents the results of our testing and analysis of the effects of array configuration on classification performance.

The upgraded EMI array performs as well in salt water as it does on land. Transmit currents are lower than planned (8.3 vs 20 A), due to limitations in the plan to modify the original transmitter. Additionally, York River noise levels encountered experimentally are 2-3x larger than those seen in air, on land during our testing at Blossom Point. To improve SNR to the levels required to meet the project's design goals would require ~800 A·turns versus the original design 480 A·turns, or the obtained 110 A·turns. This could be achieved by either: a) new transmitter loops with heavier gauge wire (*e.g.*, 80 turns of 6 AWG wire), or b) a new bipolar transmitter capable of using higher supply voltages (*e.g.*, +/- 48 Volts).

Contents

Figures

Acronyms

cDAQ	Compact Data Acquisition System
EMI	Electromagnetic Induction
ESTCP	Environmental Security Technology Certification Program
MTA	Marine Towed Array
NRL	Naval Research Laboratory
RMS	Root-Mean-Square
Rx	Receive
SERDP	Strategic Environmental Research and Development Program
SNR	Signal to Noise Ratio
TEM	Transient Electromagnetic
TEMTADS	Transient Electromagnetic – Multi-sensor Towed Array Detection System
Tx	Transmit
UXO	Unexploded Ordnance
VIMS	Virginia Institute of Marine Science

Objective

Many active and former military installations have ranges and training areas that include adjacent water environments such as ponds, lakes, rivers, estuaries, and coastal ocean areas. At other sites, training and testing areas were deliberately situated in water environments. Disposal and accidents have also generated significant munitions contamination in the coastal and inland waters in the United States. On land, the Environmental Security Technology Certification Program (ESTCP) Classification Pilot Program has demonstrated that the advanced electromagnetic induction (EMI) sensor arrays emerging from research sponsored by the Strategic Environmental Research and Development Program (SERDP) and ESTCP can be used to reliably detect and classify buried unexploded ordnance (UXO) at real munitions response sites under operational conditions. They are currently undergoing transition to commercial munitions response projects. A comparable capability does not exist for UXO detection and classification at underwater sites.

The Marine Towed Array (MTA) is an underwater dual-mode sensor array that was designed and developed over multiple years with funding under SERDP project MR-1322 [1] and ESTCP project MR-200324 [2]. It combines an array of eight magnetometers with an EMI array based on Geonics EM38 technology and comprising a 4.6 m by 1.0 m transmit (Tx) coil with four 1.1 m by 0.5 m receive (Rx) coils. The magnetometer array has been successfully used for underwater target detection and location at a number of sites (former Duck NC Naval Target Facility, former Puget Sound WA Naval Ammunition Depot, former Erie OH Army Depot, Vieques and Culebra PR, the Potomac River off Blossom Point MD and San Diego CA harbor). The EMI component was never properly evaluated. In the first MTA demonstration at the former Duck Naval Target Facility, the data were contaminated by noise created by a synchronization problem in the data acquisition software [3]. Following that demonstration, the EMI array system was redesigned in an attempt to improve performance, but initial measurements in the next demonstration (Puget Sound - Ostrich Bay) revealed that the signal-to-noise ratio (SNR) level was once again compromised [4]. The EMI array failed due to a flooded interface module shortly thereafter and was never successfully deployed again [5].

The objective of this project is to replace the existing EMI array with one based on advanced electronics and sensor designs and evaluate its classification performance. This report documents the final fabrication and integration of the full-sized EMI array and the results of our testing and analysis of the MTA performance in general and specifically, the EMI array classification performance. The project plan includes a Go/No-Go decision point following completion of this testing and analysis. Our results indicate that all systems function as well in the marine environment as they do in air, on land. Due to transmit current limitations and further limited by measured environmental noise levels, we do not recommend that the project move forward to a full demonstration.

Technical Approach

The MTA tow body (shown on a trailer to NRL's Blossom Point test facility in the photograph on the left in Figure 1) is a 4.8 m wide wing-shaped fiberglass structure designed to be towed from a medium size (~30 ft) utility vessel. Elevators on the trailing edge are driven by a control system to maintain a fixed height above the bottom during normal operations. The diagram on the right in Figure 1 shows the original MTA EMI array configuration. The transmit coil is 4.6 m wide and 1.0 m long and has 24 turns carrying a nominal current of 20 A. There are four 1.1 m by 0.5 m receiver coils, each with 56 turns. The electronics is based on the Geonics model EM38 transient electromagnetic (TEM) sensor. The transmitter is operated in a bipolar mode at 7.5 Hz and data are recorded from each of receiver coils into 26 log-spaced, time-delay bins spanning the range from 0.1 ms to 32 ms after the transmit current cutoff.

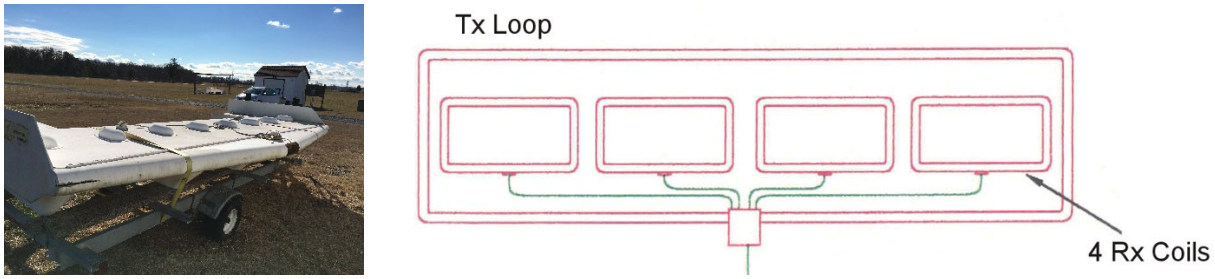

Figure 1. (left) The Marine Towed Array tow body on a trailer at NRL's Blossom Point test facility. (right) Diagram of existing MTA EMI array configuration.

The existing EMI sensor array is based on 1990's EMI technology with analog electronics which has proven to be inadequate for reliable classification work. SERDP- and ESTCP-sponsored work over the last fifteen years has shown that arrays which combine single axis transmitter coils with multi-axis receivers and are controlled using modern digital electronics can be used to reliably detect and classify UXO. The objective of this project is to replace the MTA's original EMI array with modern EMI sensors and electronics and use the new system to evaluate detection and classification performance in the underwater environment.

The MTA typically flies 1 - 1.5 m above the bottom [6]. With the standard cart-based TEMTADS 2x2 system developed in ESTCP project MR-200909 [7] the sensors are nominally 20 cm above the ground. All things being equal, increased standoff translates directly to decreased signal levels, degrading performance. Due to its larger size the MTA transmit coil has a larger transmit moment than the TEMTADS 35 cm transmit coils. This increases signal strength, compensating for the loss due to increased standoff distance. The performance dividend which results from a large transmit coil was recognized during the development of the MTA [1, 3]. The effect is illustrated in Figure 2. The solid blue curve shows how the amplitude of the TEMTADS signal (at 0.3 ms following primary field cutoff) decays with range for a target (in this case a 105 mm projectile) in its minimum signal orientation. The points are measured signals

for various target orientations, and the horizontal dashed line is a representative (Camp Spencer) RMS noise level for the TEMTADS 2x2 in survey mode. Results of a similar calculation using MTA transmit coil parameters are shown by the chain-dashed black line. The larger MTA transmit coil extends the range at which the signal drops to noise level by more than the increased standoff range of the MTA sensor array relative to the TEMTADS array.

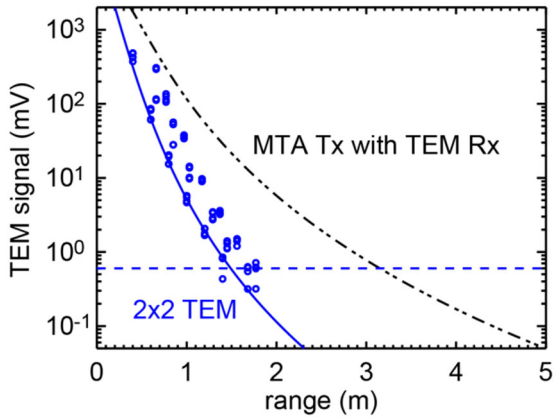

Figure 2. TEMTADS 2x2 signal vs. range response curve for a 105 mm projectile (0.3 ms following the primary field cutoff) compared with the corresponding response curve calculated using the MTA transmit coil parameters. Symbols are measured TEMTADS signals, and the horizontal dashed line is a representative survey mode noise level.

EMI-based classification uses target features (principal axis polarizabilities) extracted from data collected with an array of receiver coils and multi-axis target illumination by some arrangement of transmitter coils. In general, a single large transmit coil passing over a target does not illuminate that target along three orthogonal axes.

Previously in this project, we have examined the classification performance of different MTA transmit coil configurations using a half-scale model array which is shown in the photograph on the left in Figure 3. The diagram on the right shows the configuration of transmit and receive coils. There are three transmit coils: a pair of 0.5 m by 1.14 m coils (Tx2 and Tx3) inside of a 0.53 m by 2.34 m outer coil (Tx1). Each has 14 turns. The current is nominally 4 A for the inner coils and 3.5 A for the outer coil. There are six 8-cm, 3-axis receive cubes spaced across the array, which is controlled with a G&G Sciences cDAQ electronics package. We refer to this as the miniMTA. All of the target signal data were collected using 2.77 ms decays with 20% gate width. Noise data were collected in full wave mode (2 μs sampling interval) with 2.77 ms decays.

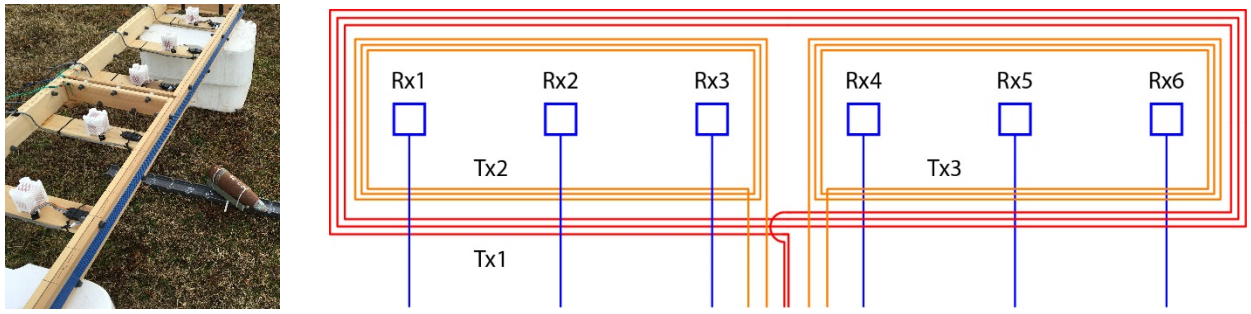

Figure 3. One-half scale model of the miniMTA EMI array used for design validation.

Data collected with the miniMTA were used to validate array performance models [8]. These were then combined with background response models validated in SERDP project MR-2409 and used to evaluate the performance of a full-scale array towed 1–1.5 m above the bottom.

Based on the results of the miniMTA analysis, the full-sized EMI array was constructed along with an updated electronics bottle. The modifications necessitated some modification to the MTA wing internal structure as well. The original and updated geophysical sensor configurations are shown schematically in the MTA wing in Figure 4. Transmitter loops are shown in green (main) and blue (inner). Total-field magnetometers are shown as blue circles and the triaxial receiver cube are shown as orange ovals.

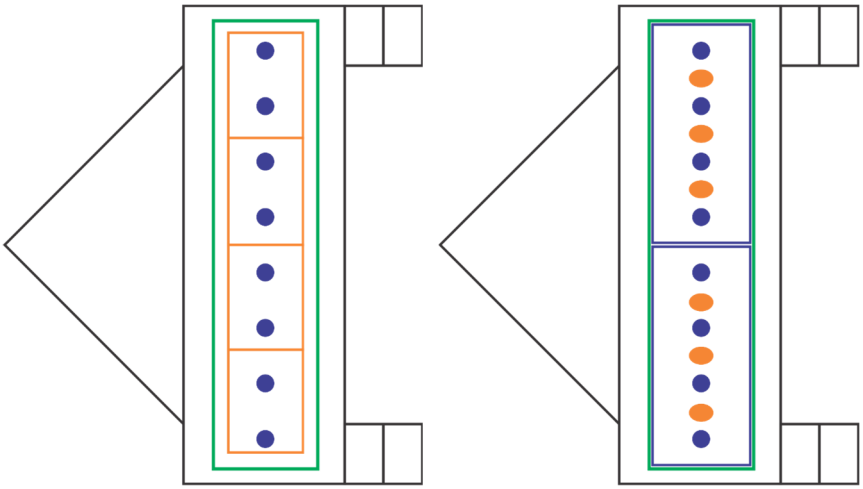

Figure 4. (left) Original MTA sensor configuration, (right) Updated MTA sensor configuration.

Full-sized EMI transmitter loops were designed to fit in the MTA wing while maximizing the generated transmit current. Based on the lessons learned from SERDP Projects MR-2409 and MR-2500, and from ESTCP Project MR-201313, a buffer area of non-conducting epoxy as insulation was added around each transmitter coil. This buffer is necessary to limit noise generated from the interactions of the loops with a conductive media (*e.g.*, sea water). The fabrication process used for the coils is shown for a small-scale example in Figure 5.

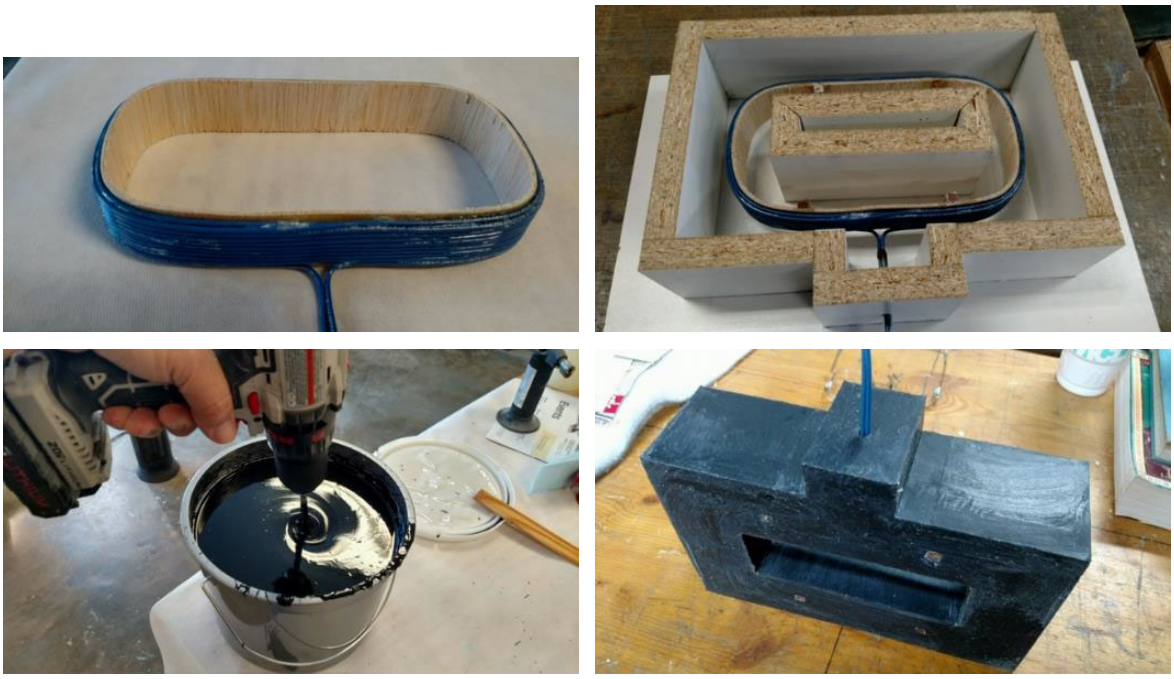

Figure 5. (upper left) Sample EMI coil winding, (upper right) Sample EMI coil suspected in form, (lower left) Waterproof epoxy being mixed, (lower right) Final sample coil released from mold.

Each loop consists of 20 turns of 14 AWG copper wire. Individual turns were carefully wound, like was done with the mini-MTA, on structural forms. A sealant was then poured into the molds around the forms and wires. Final coil dimensions were: Main loop: 4.63 m x 1.07 m; Inner loops: 2.26 m x 0.97 m.

After installation of the transmitter coils and the triaxial receiver cubes, in waterproof housings, the full-sized array was tested first in air, on land at our facility in Welcome, MD in August, 2019. After characterization, the entire wing was sent to VIMS in Gloucester Point, VA for in-water testing with emplaced UXO surrogates in September, 2019.

Figure 6. (left) MTA with EMI array installed, (center) Sphere rolling test, (right) Close-up of MTA showing magnetometers, receiver housings, and transmitter loops.

Data near VIMS were collected over a test strip during the period of low tide from noon to 3:30 PM on September 26th upriver from 37.257° N, 76.514° W. The test site is indicated by the yellow pin shown in Figure 7(a). The water depth was 6.7 m, and the water column was weakly stratified with an average conductivity of 3.45 S/m. The array was towed behind the *R/V Tidewater*, shown in Figure 7(b), at a nominal speed of 1 m/s with roughly 20 m of tow cable.

The test strip was comprised of six targets attached to a rope line stretched between a pair of anchors a distance of 102 m apart, shown schematically in Figure 8. The targets, shown in Figure 7(c), were spaced at 10 m intervals in the middle of the line. There were two 12-in diameter hollow steel balls (wall thickness 1/8-in, drilled through), two 4-in diameter by 12-in long steel pipe sections (105mm projectile surrogates) and two 6-in diameter by 18-in long steel pipe sections (155mm projectile surrogates). The 105mm surrogates are the large industry standard objects (LISO) referred to in the Geophysical System Verification documentation [9]. We will refer to the 155mm surrogates as extra-large industry standard objects (XLISO). The EMI response of the sphere is comparable to the transverse response of the XLISO.

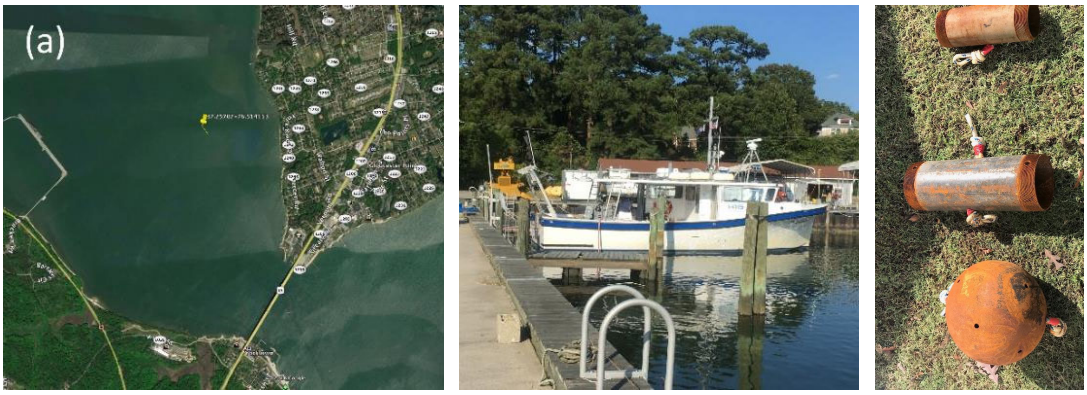

Figure 7. (left) Test site near VIMS, (center) *R/V Tidewater*, (right) UXO surrogates used.

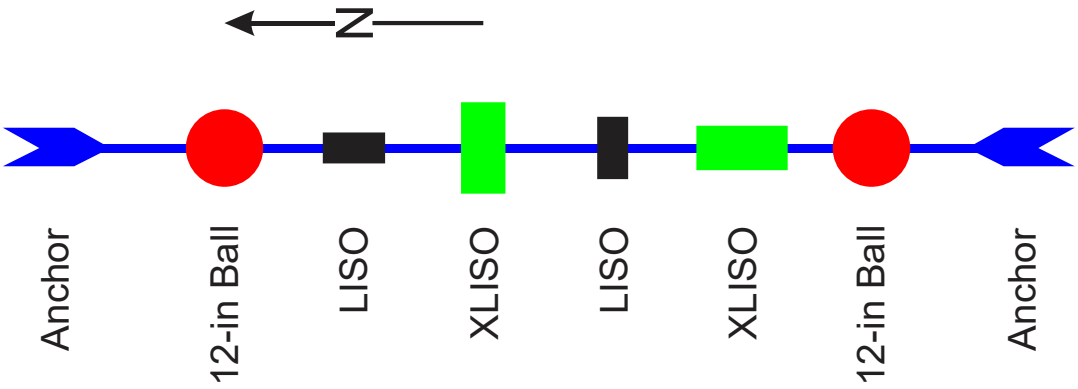

Figure 8. Schematic of York River test strip

Results and Discussion

The basic characteristics of the MTA array response were characterized on land at our Blossom Point, MD facility prior to operating the MTA in the water. Following the evaluation methods used previously for the miniMTA, dynamic data collection was simulated two ways. First, by observing the response from each of the receivers in one half of the array as a 12-in diameter steel ball was rolled along a fiberglass rail placed across the array as shown in Figure 6 (center). The rail was placed above the receiver cubes and transmitter loops, and forward of the receiver cubes so that a response would be observed in all three axes of the receiver cubes.

The observed responses for all of the data channels are shown in Figure 9 and Figure 10. Responses for receiver cubes Rx1 – Rx6 are shown by the red, orange, yellow, green, blue and violet curves, respectively. In Figure 9, the sphere passes over Tx3 and Rx1, Rx2, Rx3. In Figure 10, the sphere passes over Tx2 and Rx4, Rx5, Rx6. The plots are arranged as follows. The left-hand column of plots shows responses in the X-direction, the center column of plots shows responses in the Y-direction and the right-hand column of plots shows responses in the Z-direction. The top row shows responses to Tx1 (the large outer coil), the middle row shows responses to Tx2 (the smaller coil enclosing cubes 4-6) and the bottom row shows responses to Tx3 (the smaller coil enclosing cubes 1-3). The ball is roughly 60 cm above the array and offset 25 cm from the array centerline. With Tx1, there is a strong response in each receiver axis as the ball passes each cube. With Tx2 and Tx3 there is a correspondingly strong response in each of the cubes enclosed within their respective coils. With the six receive cubes like this, either the outer transmit coil (by itself) or the inner Tx pair can serve to detect and locate targets. At issue is their classification performance. For comparison, the results of similar testing from the miniMTA are shown in Figure 11.

Secondly, classification performance was evaluated by placing a target in a series of fixed positions along the X-direction (perpendicular to the array) under the array, collecting several hundred data points at each position, inverting the data using the standard dipole response model [11], and then comparing the principal axis polarizabilities from the inversion with corresponding polarizabilities from the standard munitions library assembled in ESTCP project MR-201424 using the UX-Analyze library matching procedure [10].

The target (item 105mmP ATC#006_HE-M1 in the ESTCP MR-201424 library) was placed on the ground, lying flat and parallel to the array. The target run consisted of sixteen measurements of the response at 30 cm intervals as the target was moved in from 4.98 m behind the array to 18 cm behind the array centerline, trailing behind Rx4. The rail was oriented perpendicular to the array in the X-direction. In this case the center of the array was nominally 66 cm above the center of the target. Data were collected using dynamic mode with the standard 2.77 ms decay and 20% gate widths. Each measurement represents an average of about 300 points. The results are shown in Figure 12.

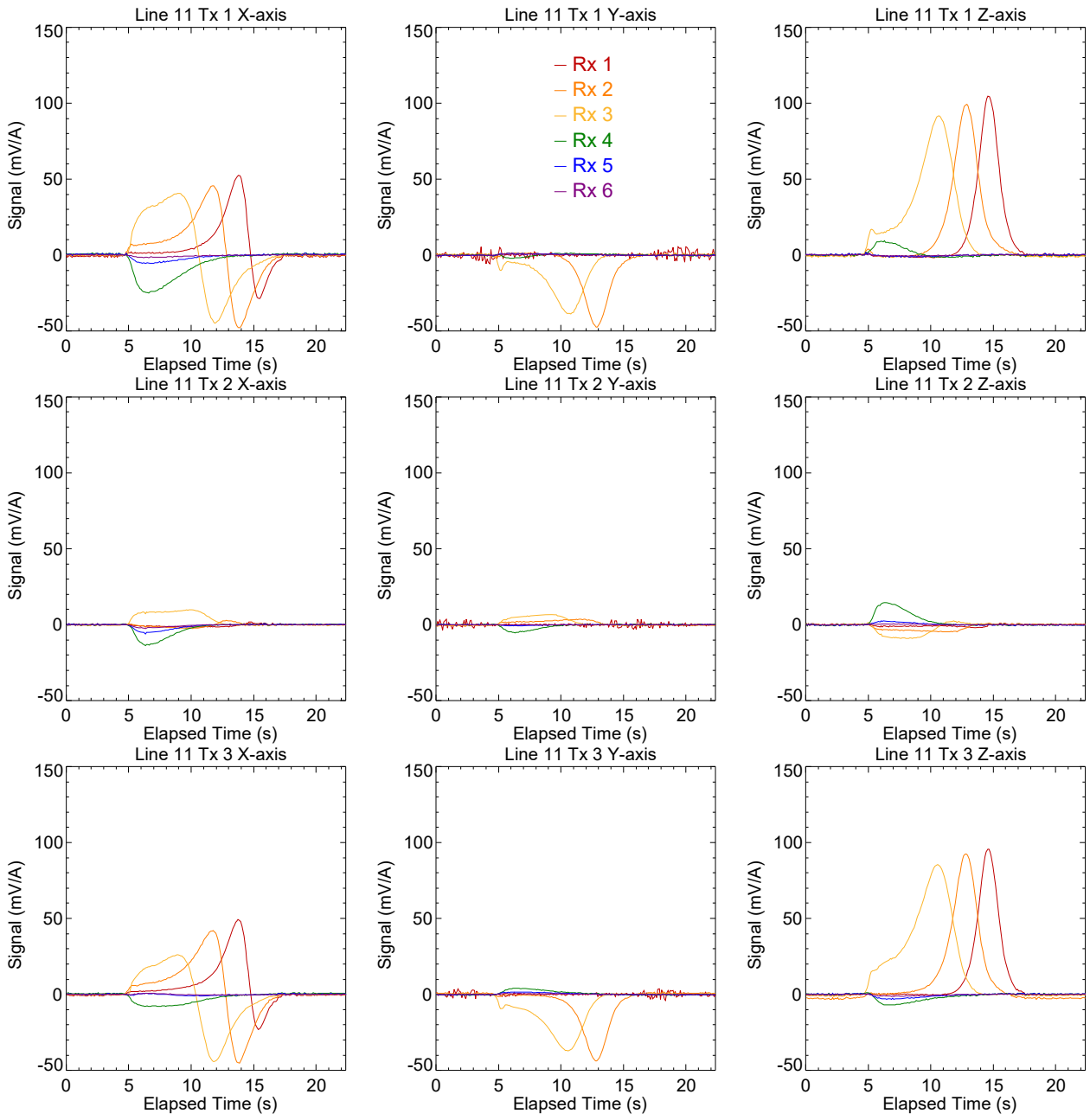

Figure 9. Measured response as a 12-in diameter steel ball is rolled along a rail above the MTA array. Responses for receiver cubes 1-6 are shown in red, orange, yellow, green, blue and violet. The ball is roughly 60 cm above the array and offset 25 cm from the array centerline.

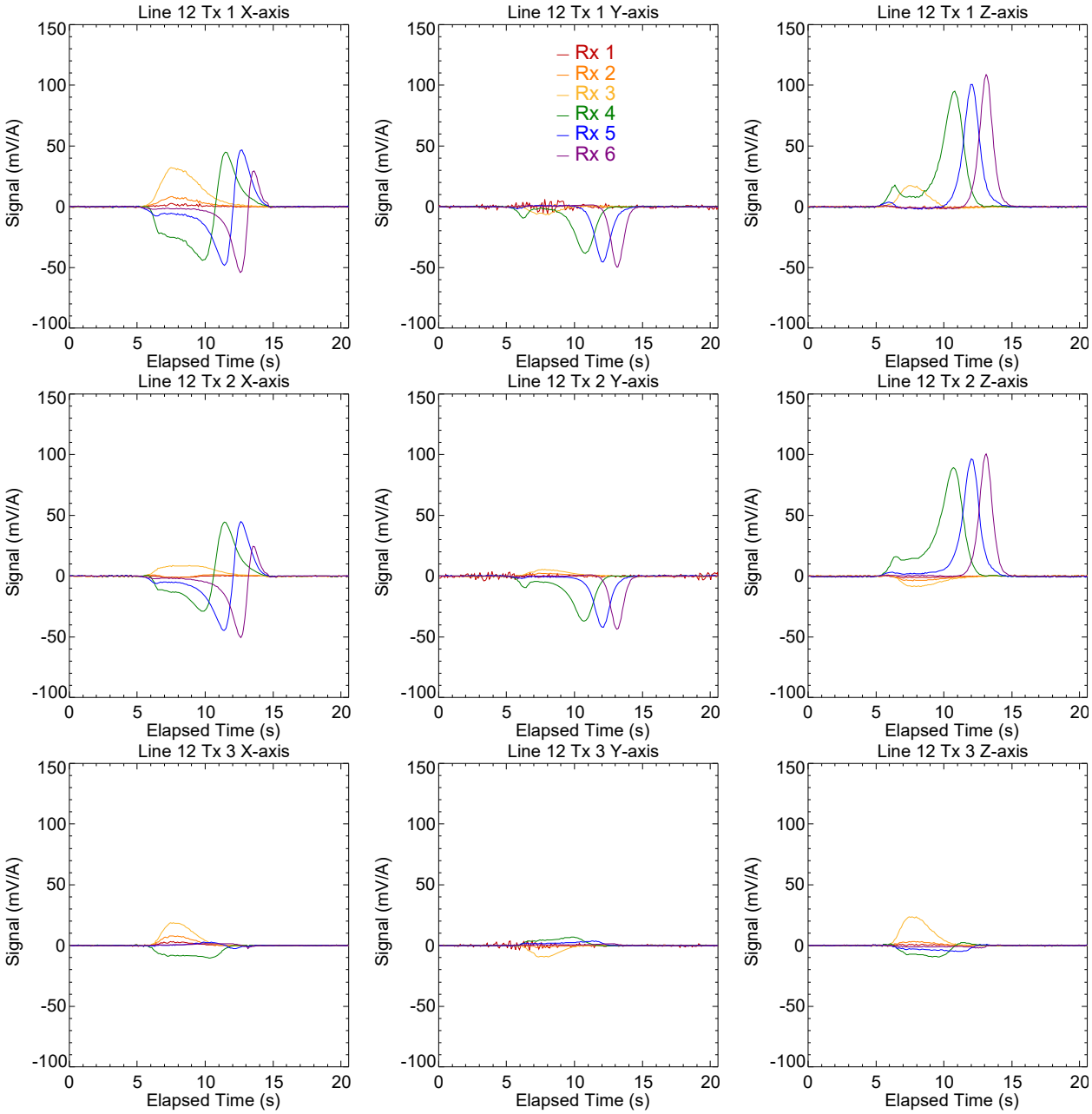

Figure 10. Measured response as a 12-in diameter steel ball is rolled along a rail above the MTA array. Responses for receiver cubes 1-6 are shown in red, orange, yellow, green, blue and violet. The ball is roughly 60 cm above the array and offset 25 cm from the array centerline.

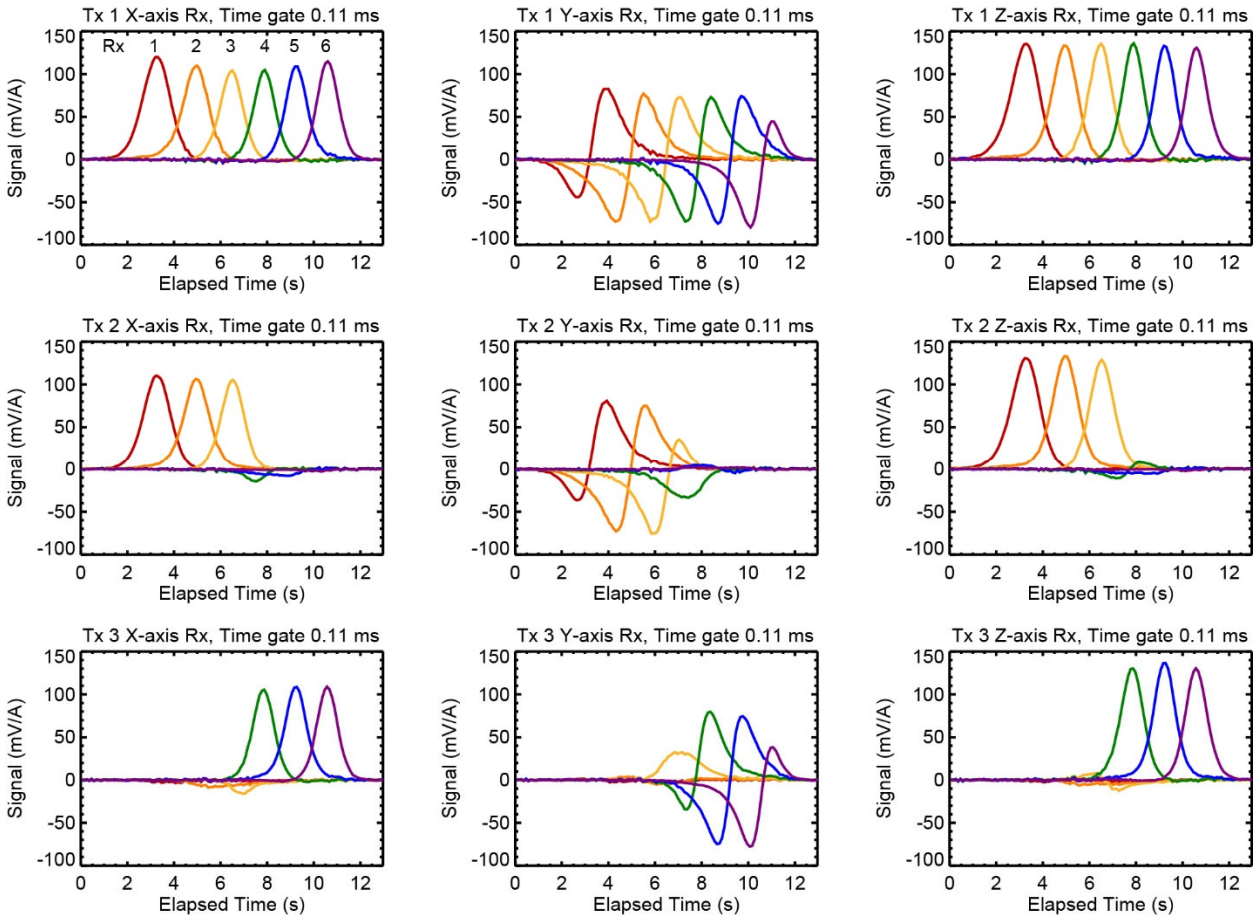

Figure 11. Measured response as a 15 cm diameter aluminum ball is rolled along a rail across the miniMTA array. Responses for receiver cubes 1-6 are shown in red, orange, yellow, green, blue and violet. The ball is roughly 20 cm above the array and offset 20 cm from the array centerline.

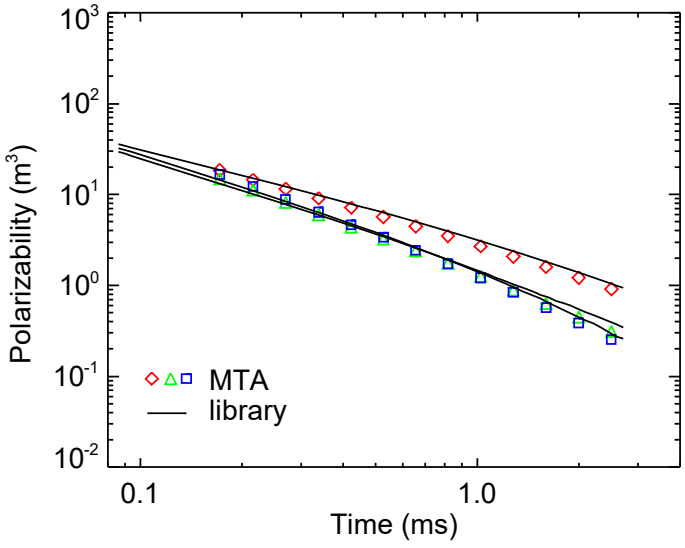

Figure 12. Inversion results for a 105mm projectile, data collection simulating a dynamic collection pass under the MTA. The black lines represent the corresponding library polarizabilities**.**

Based on these results, it was determined that all elements of the array were functional, but that the transmit currents that could be achieved with the existing configuration did not meet the design goal. In consultation with the transmitter manufacturer, it was determined that the original modification plan for the standard cDAQ EMI transmitter from nominally 6 to nominally 20 A was not feasible with the new, larger EMI coils.

The transmitters used in the TEMTADS family of AGC systems operate in a bipolar transmission mode to suppress 60 Hz noise. The overall transmitted current first contains a positive-going current pulse, followed by a decay period, followed by a negative-going current pulse, and a second decay period. The stacking process then inverts the response from the "negative" decay, and adds it to the "positive" decay. Three supply voltages are input to the transmitter electronics to support this mode of operation: a ground for reference and two equal but opposite signed voltages, +V and –V. The nomenclature +/-V will be used for the remainder of this document, for example, +/-15 VDC corresponds to the standard TEMTADS supply voltages of +15 VDC, ground, and -15 VDC.

The transmitter was modified to operate on +/-24 VDC supplies, up from the standard +/-15 VDC supplies. Increasing the supply voltages to the transmitter directly increases the transmitter output current, as shown in Figure 13 (a). However, without serious risk to the transmitter itself, the manufacturer recommended not increasing the supply voltage beyond +/-24 VDC. At this supply voltage, the transmit current achievable are main (outer) loop to 5.7 A, and to 8.3 A in the inner loops. As a window of opportunity was available in September for in-water testing, the team determined that comparing the in-water performance of the EMI array to the land-based performance was more valuable than the potential of damaging the transmitter electronics by pushing the supply voltage further.

The array was moved to VIMS for staging into the York River in September, 2019. The vessel captain piloted the R/V along the line between the two anchor points using his on-board navigation display in both directions (along the line). Fifteen passes along the test strip were run with the array at nominal altitudes above the bottom ranging from 0.75 m to 1.5 m. Layback calculations for reconstructing the array trajectory which were part the original data acquisition system were not available for this test. Signals were registered for 33 of the 80 possible target encounters. For 28 of these the target passed under the array and the remaining 5 targets passed nearby, off to the side of the array.

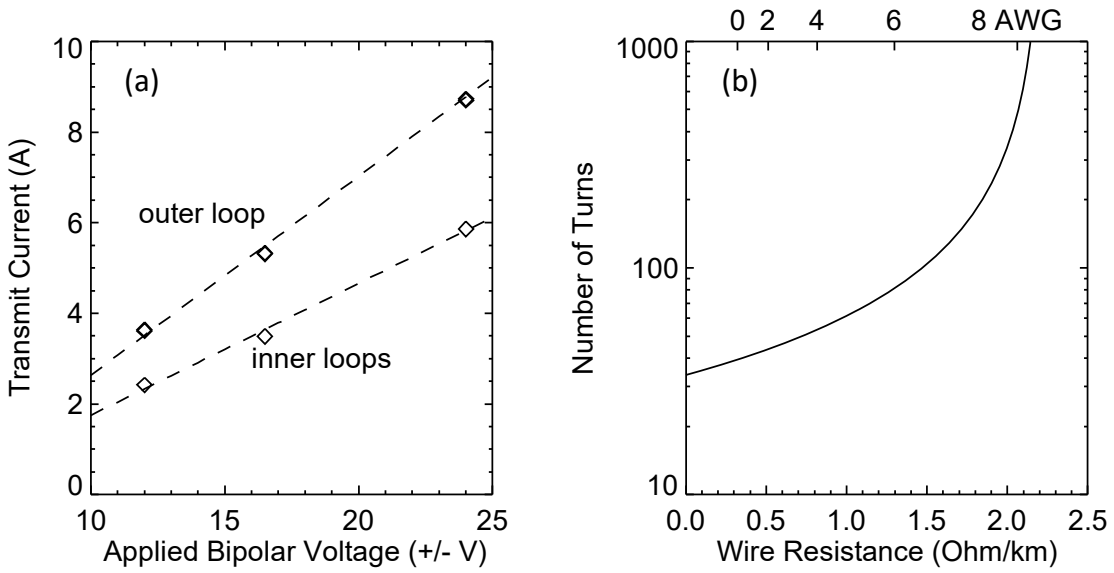

Figure 13. (a) Transmit current vs. applied bipolar voltage for MTA EMI array (see text for discussion of voltage nomenclature). (b) Number of turns and wire resistance need to achieve 800 A·turns of transmit current in the main (outer) loop.

Figure 14(a) is a scatter plot of signal strength vs. array height above the bottom for the 28 targets which passed under the array. The plotted signal strength is the maximum Z-axis response at 0.216 ms from the main transmitter loop on any of the cubes. The signal strength depends on where the target passes under the array, being strongest when the target passes directly under one of the receiver cubes towards the center of the array, is weaker when the target passes under the array between two cubes at the closer ranges. The dashed lines are response curve calculations intended to bound the measurements and show that the array performed as expected. The lower curve is the signal expected for a 105mm projectile lying flat on the bottom which passes under the array between two of the receiver cubes. The upper is for a 155mm projectile passing under one of the cubes. Expected signal vs. range was calculated using the standard dipole response model [11] with library polarizabilities [12] for 105mm M1 and 155mm M107 projectiles.

One note is that change in starting decay time from the miniMTA work at 0.1ms to the 0.216ms used here. Stronger early time saturation, primarily lasting later in time, was observed with the full array than was seen with the miniMTA array. Removal of the magnetometers improved the early time saturation significantly, but did not reduce it to miniMTA or TEMTADS 2x2 levels.

The data were inverted to determine target location, orientation and polarizability using the standard dipole response model [11]. We used a four-meter stretch of data from over each target. The background response was subtracted using the average response of adjacent four-meter stretches. Figure 14(b) shows inversion fit quality vs. signal strength for the targets. Fit quality is the correlation coefficient between the data and the model fit to the data. The dashed curve shows the expected behavior of this metric as a function of signal strength:

$$Fit\ Quality = S/\sqrt{S^2 + N^2}$$

where S is the signal and N is the noise. The curve is a universal function of signal to noise ratio (SNR). The peak signal is a proxy for the array SNR in this case. The agreement between the model curves and the data in Figure 14 shows that the array is performing as expected.

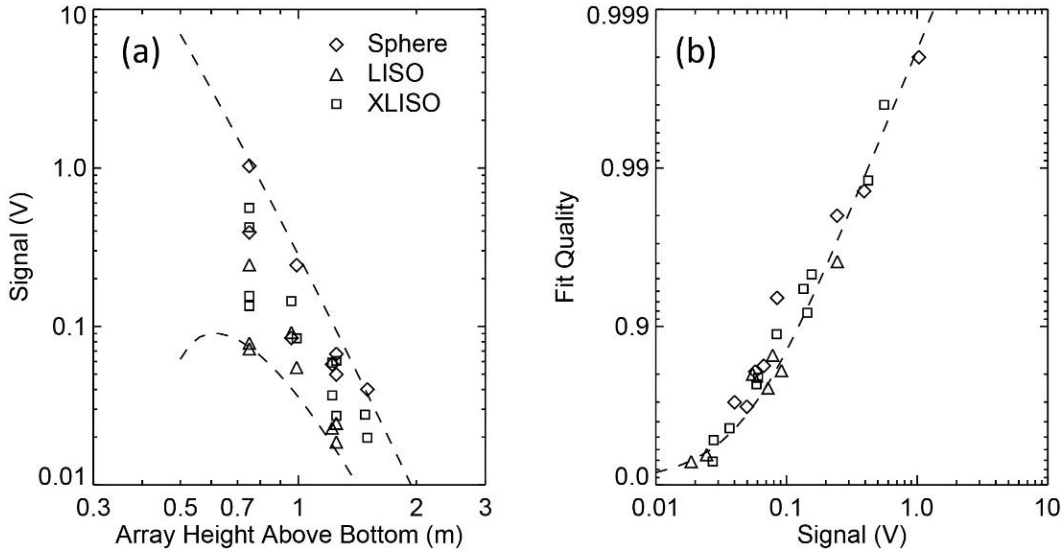

Figure 14. (left) signal strength vs. array height above the bottom for detected targets. The dashed lines bound the expected responses for a 105mm projectile lying flat on the bottom which passes under the array between two of the receiver cubes and for a 155mm projectile passing under one of the cubes. (right) Inversion fit quality vs. signal strength for the targets. The dashed curve shows the expected behavior of this metric as a function of signal strength.

With the array fielded, we get good estimates of the target polarizabilities with fit qualities of roughly 0.75 and higher. Figure 15 and Figure 16 show examples. Figure 15(a)-(d) are for the hollow steel ball at nominal array heights of 0.75 m, 1.0 m, 1.25 m and 1.5 m above the bottom. The symbols show the polarizability determined by inverting the array data and the curves are the expected polarizability calculated from formulae derived by Hjelt [13], using a conductivity of 5 x 10^6 S/m and a relative permeability of 100. Our calculation accounts for the short pulse run-on and the 0.039 ms time lag in our electronics. The inversion fit quality is 0.998, 0.980, 0.837 and 0.617 for Figure 15 (a) through (d), respectively, with corresponding signal strengths of 1.03 V, 0.24 V, 0.056 V and 0.040 V. Deviations between the data-derived and actual (calculated) polarizabilities are less than 15% for the first three (with fit quality greater than 0.8), but 88% for the final one which has a fit quality less than 0.7. Figure 16 shows results for the LISO. Here the curves are library polarizabilities. The nominal array heights are 0.75 m and 1.0 m above the bottom, respectively. Fit quality and signal strength are as noted on the plots. The target passed under the starboard edge of the array in Figure 16(a) and near the center in Figure 16(b). Deviations of the data-based polarizabilities from the library polarizabilities are 17% and 15% in these cases.

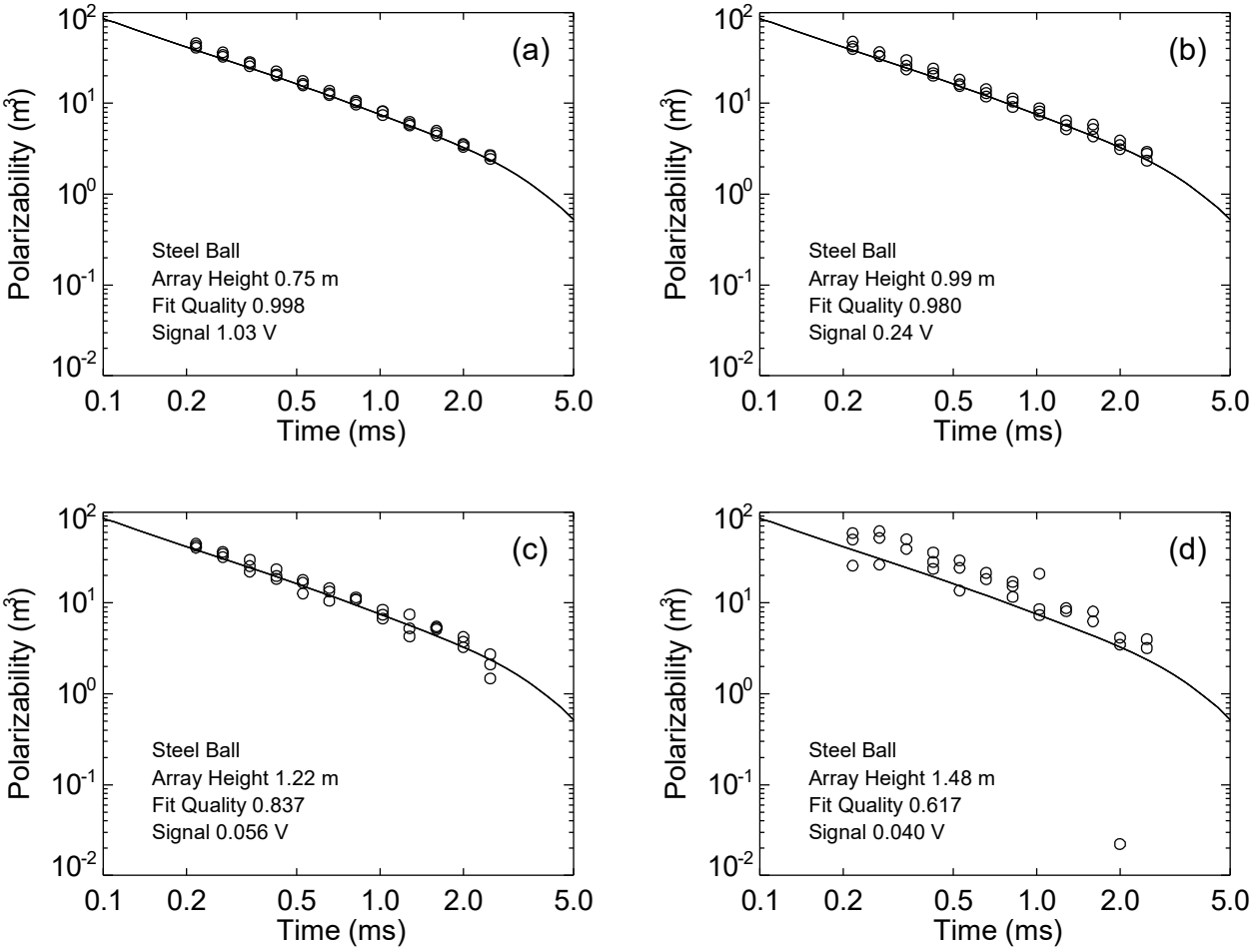

Figure 15. Examples of polarizabilities determined by inverting array data. Symbols are measured polarizability, curves are calculated (sphere).

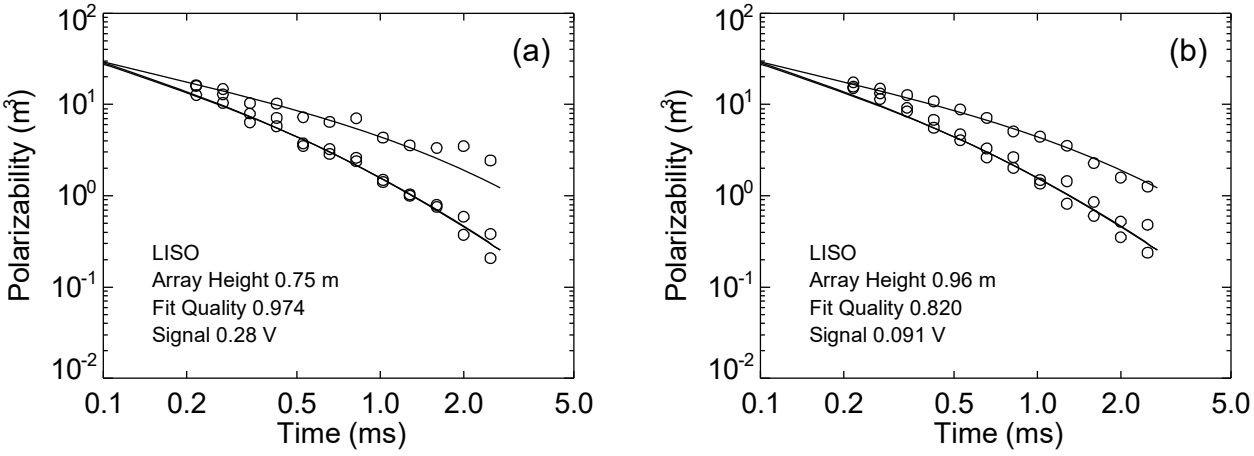

Figure 16. Further examples of polarizabilities determined by inverting array data. Symbols are measured polarizability, curves are library polarizabilities for an LISO.

The root mean square (RMS) noise level during the test was 2.3 mV at the 0.216 ms time gate. This is comparable to noise levels observed at other stations along the York River in the summer of 2016 using a standard TEMTADS/3D transmit coil – receive cube pair [14] encased in a Delrin pressure housing and a second receive cube (offset horizontally by 35 cm) in a pressure housing like those shown in Figure 17. The data were collected during a study of background EMI response in marine environments conducted as part of Strategic Environmental Research and Development Program (SERDP) project MR-2409 [15]. The MTA EMI array design study used a noise model based on in-air data collected with a one-half scale model at the Blossom Point test site and an assumed transmit current of 20 A [8]. The corresponding RMS noise level for these data was 0.69 mV. As presently configured the main loop of the array has 20 turns and carries a current of 5.7 A (114 A·turns). Based on the performance models used to produce the curves in Figure 14, with noise levels in the 2-2½ mV range we would need about 800 A·turns to classify 105mm projectiles at a range of 1.5 m.

New transmit coils could be built to accommodate 800 A·turns with the current ±24 V system. Measurements of the transmit current in the MTA EMI loops at different applied voltages are plotted in Figure 13(a). The dashed lines show the current – voltage relationship

$$Transmit\ Current = \frac{Applied\ Voltage - \delta V}{R_0 + n\rho L}.$$

δV = 4 V is a voltage drop across the diode switches, n = 20 is the number of turns in the transmit loops, L = 6.25 m and 11.28 m are the circumferences of the inner and outer loops, R_0 is the residual resistance in the circuit and ρ is the resistance per unit length of the wire in the loops. The data are fit with R_0 = 0.84 Ω and ρ = 11.5 Ω/km. Figure 13(b) shows the number of turns vs. wire resistance required to achieve 800 A·turns with an applied voltage of ±24 V. The AWG scale corresponding the wire resistance values is shown at the top. 6 AWG seems to be the best choice based on the cross-sectional area occupied by the windings. 81 turns are needed for 800 A·turns. The available space for the coils is 7 cm high, and the windings are embedded in potting material which extends 2 cm out from the wires in all directions. Heavy-build 6 AWG film-insulated magnet wire (Superior Essex, Inc.) has a diameter of 0.42 cm. 85 turns of this wire could be wound in a bundle 3.8 cm high by 3.7 cm wide.

Another option for achieving the desired 800 A·turns would be modification / replacement of the transmitter itself. Based on discussions with G&G Science, two issues for moving in this direction with the existing transmitter are a) the need to replace the IBGT switches with ones rated for higher voltages. As the transmit current increases, the voltage drop across these switches increases.

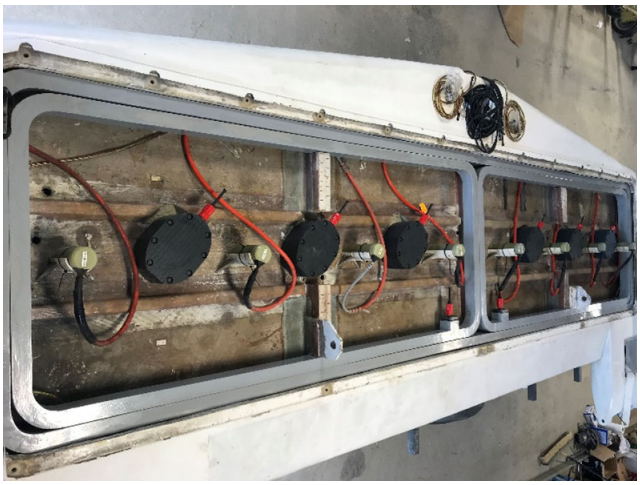

Figure 17. Interior of the marine towed array. Rounded gray rectangles are transmit loops, black ovals are pressure housing containing receiver cubes and green cylinders contain magnetometers.

For example, TEMTADS 2x2 system has to incorporate a 1Ω resistor into the transmitter circuit to keep the voltage across the IGBTs (several hundred volts) below the damage threshold to use the standard 16VDC version of the Ultralife UBI-2950 batteries, where the resistor is not required to use the non-standard 12VDC version. The second issue is the voltage ratings of the other electronic components (*e.g.*, DC/DC power supplies) were specified in the 24 – 32 volt range and would likely need to be uprated to support higher supply voltages. Along these lines, sourcing a transmitter with higher power and similar temporal response could resolve the issue, but could potentially cause integration issues into the pressure vessel. It was suggested during the most recent IPR that the transmitter could be moved to the boat, removing the integration issue, but this offers additional logistical issues of separating the transmitter from the control logic (which needs to remain near the receivers for noise issues).

Increased transmit moment should not affect the receiver noise. Figure 18 shows ungated, full-wave root-mean-square (RMS) noise levels *vs.* transmit moment for various transmit coils tested in SERDP project MR-2409 [16] (diamonds) and the miniMTA coils with battery voltages of 12 V and 15 V (squares). There is no significant trend above the normal day-to-day variations.

Based on the results of our land-based and in-water testing, a full-scale demonstration is not recommended for this array. The useful standoff distances are too small to be practical for survey work, basically requiring the array to travel at the bottom level to see a 105mm projectile buried to a depth of 1.5m. The updated wing and EMI array are fully functional. In-water performance is nominal as compared to land-based performance, further indicating that there is no physics-based barrier to the use of EMI sensors and AGC methodologies in the marine environment.

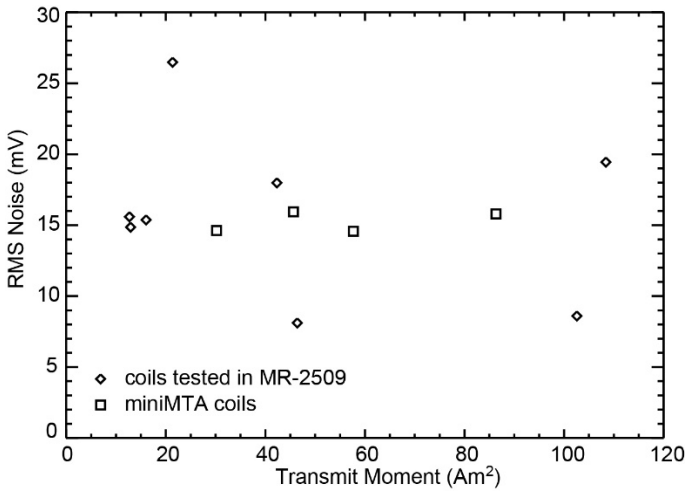

Figure 18. RMS noise (ungated full-wave) *vs.* transmit moment for the various transmit coils tested in MR-2409 (diamonds) and the miniMTA coils (squares).

We recommend a final effort to explore some of the remaining fundamental questions about EMI compatibility with marine environment. For example, we suggest exploring the results for larger targets at greater range, where environmental signal distortion will play a more significant role. Additionally, it would be informative to explore large non-axisymmetric (*i.e.*, clutter) items. We would like to briefly investigate the source of the early time saturation issue further. Removing all non-essential metal (*e.g.*, magnetometers) from the proved a start in this direction.

Conclusions

The upgraded EMI array performs as well in salt water as it does on land. Transmit currents are lower than planned (8.3 vs 20 A), due to limitations in the plan to modify the original transmitter. Additionally, York River noise levels encountered experimentally are 2-3x larger than those seen in air, on land during our testing at Blossom Point. For reference, noise levels were 2.3 vs 0.7 mV at the 0.216 ms time gate. To improve SNR to the levels required to meet the project's design goals would require ~800 A·turns versus the original design 480 A·turns, or the obtained 110 A·turns. This could be achieved by either: a) new transmitter loops with heavier gauge wire (*e.g.*, 80 turns of 6 AWG wire), or b) a new bipolar transmitter capable of using higher supply voltages (*e.g.*, +/- 48 Volts).

Literature Citations

1. J. McDonald, “Technology Needs for Underwater UXO Search and Discrimination,” Final Report, SERDP Project MR-1322, October 2003.

2. J. R. McDonald, “UXO Detection and Characterization in the Marine Environment," Technical Report, ESTCP Project MM-200324, July 2009.

3. J. R. McDonald, “Marine Towed Array Technology Demonstration at the Former Naval Duck Target Facility,” Interim Report, ESTCP Project MR-200324, November 2005.

4. J. R. McDonald, "UXO Detection and Characterization in the Marine Environment," Final Report, ESTCP Project MR-200324, November 2008.

5. J. R. McDonald, "Demonstration of the Marine Towed Array on Bahia Salinas del Sur Vieques, Puerto Rico," Interim Report, ESTCP Project MR-200324, February 2009.

6. Robert DiMarco, Dean Keiswetter and Thomas Bell, “Deep Water Munitions Detection System,” Final Report, ESTCP Project MM-200739, March 2010.

7. James B. Kingdon, Bruce J. Barrow, Thomas H. Bell, David C. George, Glenn R. Harbaugh and Daniel A. Steinhurst, "TEMTADS Adjunct Sensor Systems: Hand-held EMI Sensor for Cued UXO Discrimination and Man-Portable EMI Array for UXO Detection and Discrimination," Final Report, ESTCP projects MR-200807 and -200909, April 2012.

8. Daniel Steinhurst, Glenn Harbaugh, and Thomas Bell, “Interim Report on Effects of Array Configuration on Classification Performance,” ESTCP Project MR-201610, March, 2017.

9. Herb Nelson, Katherine Kaye and Anne Andrews, 'Geophysical System Verification (GSV): A Physics-Based Alternative to Geophysical Prove-Outs for Munitions Response," ESTCP Report, July 2009 (Addendum September 24, 2015).

10. Dean Keiswetter, "2010 ESTCP UXO Classification Study, Camp Butner, NC," Interim Report, ESTCP Project MR-200910, April 2012.

11. Thomas H. Bell, Bruce J. Barrow, and Jonathan T. Miller, "Subsurface Discrimination Using Electromagnetic Induction Sensors," *IEEE Transactions on Geoscience and Remote Sensing*, Vol. 39, No. 6, June 2001.

12. Craig Murray, Nagi Khadr, Thomas Bell and Daniel Steinhurst, "Munitions Classification Library," ESTCP Project MR-201424 Final Report, April 2016 (Addendum September 2016).

13. S-E. Hjelt, “The Transient Electromagnetic Field of a Two-Layer Sphere,” Geoexploration, vol. 9, 213-229 (1971).

14. Herbert H. Nelson, Daniel A. Steinhurst, Glenn R. Harbaugh and Thomas H. Bell, "System for the Detection and Classification of Buried Unexploded Ordnance," United States Patent 9,651,341 B2, May 16, 2017.

15. Thomas Bell, Bruce Barrow, Daniel Steinhurst, Glenn Harbaugh, Carl Friedrichs and Grace Massey, "Empirical Investigation of the Factors Influencing Marine Applications of EMI," SERDP Project MR-2409 Final Report, March 2018.

16. Thomas Bell, Bruce Barrow, Daniel Steinhurst, Glenn Harbaugh, Carl Friedrichs and Grace Massey, "Empirical Investigation of the Factors Influencing Marine Applications of EMI: Tank Testing," Interim Report, SERDP Project MR-2409, April 2016.